

Response to reviewers' comments

Thanks to the reviewers for giving us very useful comments to improve our manuscript entitled "Modeling the impact of heterogeneous reactions of chlorine on summertime nitrate formation in Beijing, China" (acp-2018-1270). Detailed responses to reviewers' comment are list below:

Report #1

Comment 1: Qiu et al., developed a revised regional CMAQ model, by updating several chloride contained reactions, to study the impact of chloride-related heterogeneous chemistry on summer particulate nitrate formation. This work is meaningful and improved the understanding of regional nitrate pollution as well as chloride chemistry. Several comments should be addressed before publishing in ACP.

Response #1: Thanks for the positive comments on this manuscript. The suggestions are addressed in detail in the following.

Comment 2: Section 3.2, the uptake coefficient of O₃ on chloride-contain aerosol were increased by a factor of 10 and showed the importance of O₃ heterogeneous reaction and the Cl₂ budget. The increasing of O₃ uptake coefficient may also strongly affect the O₃ lifetime, an intercomparison of modeled and observed O₃ need to be conducted to verify the rationality and prove the significance.

Response #2: In previous response #3 from the reviewer #1, we have performed the comparison of predicted O₃ concentration in HET case with observation, as Table R1. We further compare the predicted O₃ concentration in uptake coefficient increased by a factor of 10 (represent as Sim* in Table R1) with observation and simulation in HET case. The results show that O₃ concentrations in 'Sim*' column are slight lower than the 'Sim' column, which may indicate that the O₃ consumption by heterogeneous reaction is generally larger than the production owing to the Cl₂ formation. Moreover, these differences are mainly found in nighttime because the weak photolysis limit the generated Cl₂ to transfer to O₃.

Table R1 Comparison of simulated 1-h NO₂, PM_{2.5} and O₃ concentrations with observations averaged from 11 to 15, June, 2017 (Obs: observation, Sim:simulation).

Sites	NO ₂				O ₃					PM _{2.5}			
	Obs	Sim	NMB	NME	Obs	Sim	Sim*	NMB	NME	Obs	Sim	NMB	NME
WSXG	49	54	11%	55%	99	122	121.6	23%	63%	40	38	-6%	53%
DL	21	17	-20%	68%	111	108	107.5	-2%	41%	32	29	-10%	52%
DS	47	53	13%	54%	100	114	113.8	15%	56%	44	41	-7%	53%
TT	40	48	20%	64%	98	130	129.4	33%	60%	37	37	1%	58%
NZG	51	66	28%	62%	111	121	120.5	9%	57%	42	39	-7%	52%
GY	55	65	17%	57%	107	116	115.4	9%	75%	36	33	-8%	54%
WL	52	41	-21%	54%	92	112	111.6	22%	73%	35	33	-7%	54%
XC	43	31	-28%	47%	100	108	107.3	8%	52%	33	29	-12%	55%
HR	26	11	-56%	70%	124	105	104.4	-15%	47%	27	22	-19%	51%
CP	42	28	-34%	58%	96	91	90.3	-5%	77%	33	32	-1%	54%
ATZX	56	62	10%	55%	105	107	106.2	1%	68%	33	31	-4%	54%
GC	56	42	-25%	58%	106	107	106.4	0%	59%	43	37	-14%	52%

38

39 WSXG: Wanshouxigong; DL: Dingling; DS: Dongsi; TT:Tiantan; NZG:Nongzhanguan;
40 GY: Guanyuan; WL: Wanliu; XC:Xincheng; HR:Huairou; CP:Changping;
41 ATZX:Aotizhongxin; GC:Gucheng

42 Sim*: O₃ concentration in uptake coefficient increased by a factor of 10

43

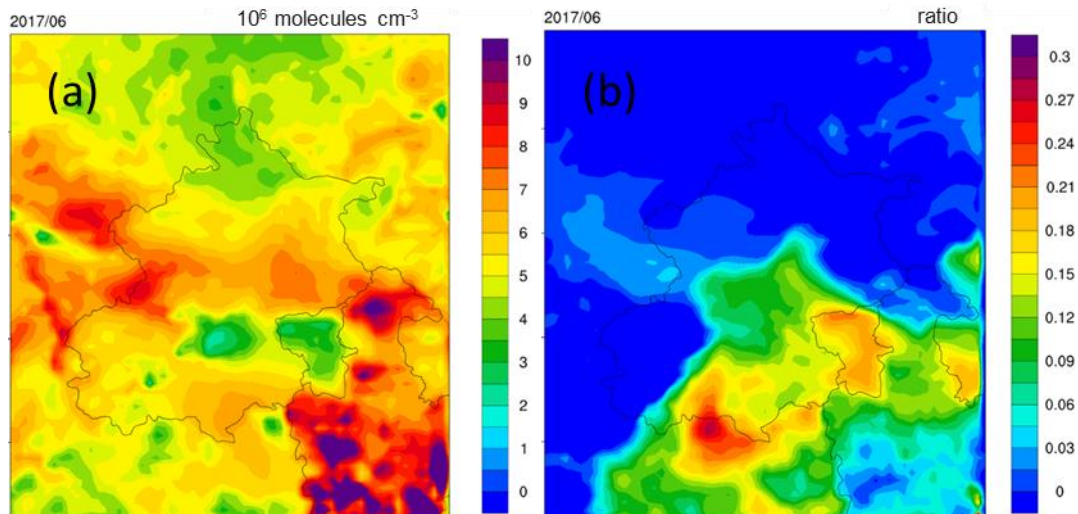
44 **Comment 3:** Figure 3(e, f) do not show the higher OH plot in Het case, so the
45 statement in line 366 can't get the conclusion that high ANO3 is attribute to the elevated
46 OH, although other studies presented the same conclusion. By the way, the photolysis
47 of CINO2 also release NO2 and enhance the reaction of OH + NO2. It would be good
48 if the increasing of daytime NO2 and OH by CINO2 photolysis can be quantified and
49 used to assess the contribution from NO2 and OH.

50

51 **Response #3:** We have supplemented the spatial distribution of diurnal OH
52 concentration (panel (a)) and difference ((HET/BASE)/BASE, panel (b)) averaged from
53 11-15 June 2017. Which can reflect that the high ANO3 is attribute to the elevated OH.
54 We add the Figure R1 in SI.

55 As the reviewer's representation, the photolysis of CINO₂ also release NO₂ and enhance
56 the reaction of OH + NO₂. However, it's hard to quantify its contribution to NO₂ in the
57 model. But we think this process can be ignored because the NO₂ generated by CINO₂
58 is rather low (because the CINO₂ is rather low, less than 1ppb). By contrast, the
59 atmospheric NO₂ concentration is reaching up to 20~40ppb.

60



61

62 Figure R1. Spatial distributions of episode-average OH concentration (a) and the
63 difference (b) from 11 to 15 June 2017. Unit: 10⁶ molecules cm⁻³

64

65 **Comment 4:** L89, high Cl- do not represent high CINO2 yield, which may be subject
66 to the aerosol liquid water content, organics and so on, please change to “When CINO2
67 yield is high...”.

68

69 **Response #4:** The sentence ‘When Cl⁻ is enough, this reaction leads to lower nitrate
70 concentrations than reaction R5.’ in line 89 is deleted.

71

72 **Comment 5:** Line 229, Eqs. 8, change to γOH .

73

74 **Response #5:** Revised.

75
76
77
78
79
80
81
82
83
84
85
86
87
88
89
90
91
92
93
94
95
96
97
98
99
100
101
102
103
104
105
106
107
108
109
110
111
112
113
114
115
116
117
118
119
120
121
122
123
124

Comment 6: Line 321, Bracket is not complete.

Response #6: Revised

Comment 7: Line 328, Tham et al., 2019 change to 2018.

Response #7: Revised.

Comment 8: Line 718-719, the font size is bigger than other words.

Response #8: Revised.

Comment 9: Line 332-336, the long sentence is difficult to read. Please divide into two sentences, "... and the larger constant N₂O₅ leads to..." change to ". The application of large and fixed N₂O₅ uptake coefficient ... "

Response #9: We have revised following the reviewer's option.

Comment 10: Line 377, subscript of "PM_{2.5}".

Response #10: Revised.

Comment 11: Figure 4 should add the base case percentage like HET in the left edge.

Response #11: The left edge in Figure 4 presents the contribution of heterogeneous reaction and HNO₃ partitioning to nitrate formation, which is concentration contribution, not the percentage.

Report #2

Comment 1: There is one thing I would like to mention, although it will not change the results and the conclusion of the present study.

In Response 35, the authors stated that "HONO photolysis affects the OH level just a few hours in the morning and can be neglected", which is not correct. It has been well established that HONO is produced both in nighttime and in the daytime, and HONO is the predominant source of OH radical during daytime (not just a few hours in the morning) in the polluted environment, e.g. Fu et al., 2019 (Fig 2 and 5) and the reference therein.

Fu, X., Wang, T., Zhang, L., Li, Q., Wang, Z., Xia, M., Yun, H., Wang, W., Yu, C., Yue, D. and Zhou, Y., 2019. The significant contribution of HONO to secondary pollutants during a severe winter pollution event in southern China. Atmospheric Chemistry and Physics, 19(1), pp.1-14.

Response #1: Thanks for the reviewer correcting our addressing. In original CMAQ, HONO is produced by the reaction NO₂ with H₂O. However, this study improves this reaction to produce ClNO and nitrate, not involve HONO. From Fu's work, there are some other HONO sources, which may increase the OH level in daytime. But we don't

125 intend to improve these to our study since our work focus on the impact of chlorine
126 heterogeneous reaction on the nitrate.
127

1 **Modeling the impact of heterogeneous reactions of chlorine on**
2 **summertime nitrate formation in Beijing, China**

3 Xionghui Qiu^{1,2}, Qi Ying^{3*}, Shuxiao Wang^{1,2*}, Lei Duan^{1,2}, Jian Zhao⁴, Jia
4 Xing^{1,2}, Dian Ding^{1,2}, Yele Sun⁴, Baoxian Liu⁵, Aijun Shi⁶, Xiao Yan⁶,
5 Qingcheng Xu^{1,2}, Jiming Hao^{1,2}

6 ¹ State Key Joint Laboratory of Environmental Simulation and Pollution Control,
7 School of Environment, Tsinghua University. Beijing 100084, China.

8 ² State Environmental Protection Key Laboratory of Sources and Control of Air
9 Pollution Complex, Beijing 100084, China

10 ³ Zachry Department of Civil Engineering, Texas A&M University, College Station,
11 Texas 77843-3138, United States

12 ⁴ State Key Laboratory of Atmospheric Boundary Layer Physics and Atmospheric
13 Chemistry, Institute of Atmospheric Physics, Chinese Academy of Sciences, Beijing
14 100029, China

15 ⁵ Beijing Environmental Monitoring Center, Beijing 100048, China

16 ⁶ Beijing Municipal Research Institute of Environmental Protection, Beijing 100037,
17 China

18 *Corresponding author: shxwang@tsinghua.edu.cn & qying@civil.tamu.edu

19 Abstract:

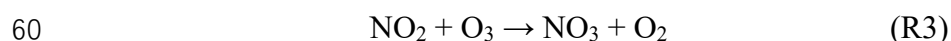
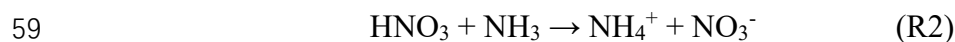
20 A comprehensive chlorine heterogeneous chemistry is incorporated into the
21 Community Multiscale Air Quality (CMAQ) model to evaluate the impact of chlorine-
22 related heterogeneous reaction on diurnal and nocturnal nitrate formation and quantify
23 the nitrate formation from gas-to-particle partitioning of HNO₃ and from different
24 heterogeneous pathways. The results show that these heterogeneous reactions increase
25 the atmospheric Cl₂ and ClNO₂ level (~100%), which further affect the nitrate
26 formation. Sensitivity analyses of uptake coefficients show that the empirical uptake
27 coefficient for the O₃ heterogeneous reaction with chlorinated particles may lead to the
28 large uncertainties in the predicted Cl₂ and nitrate concentrations. The N₂O₅ uptake
29 coefficient with particulate Cl⁻ concentration dependence performs better to capture the
30 concentration of ClNO₂ and nocturnal nitrate concentration. The reaction of OH and
31 NO₂ in daytime increases the nitrate by ~15% when the heterogeneous chlorine
32 chemistry is incorporated, resulting in more nitrate formation from HNO₃ gas-to-
33 particle partitioning. By contrast, the contribution of the heterogeneous reaction of
34

35 N₂O₅ to nitrate concentrations decreases by about 27% in the nighttime when its
36 reactions with chlorinated particles are considered. However, the generated gas-phase
37 ClNO₂ from the heterogeneous reaction of N₂O₅ and chlorine-containing particles
38 further reacts with the particle surface to increase the nitrate by 6%. In general, this
39 study highlights the potential of significant underestimation of daytime and
40 overestimation of nighttime nitrate concentrations for chemical transport models
41 without proper chlorine chemistry in the gas and particle phases.

42

43 1. Introduction

44 In recent years, nitrate has become the primary component of PM_{2.5} (particulate matter
45 with aerodynamic diameter less than 2.5μm) in Beijing with sustained and rapid
46 reduction of SO₂ and primary particulate matter emissions (Ma et al., 2018; Li et al.,
47 2018; Wen et al., 2018). Observations showed that the relative contributions of
48 secondary nitrate in PM_{2.5} could reach up to approximately 50% during some severe
49 haze pollution days (Li et al., 2018). The mechanism of secondary nitrate formation can
50 be summarized as two major pathways: (1) Gas-to-particle partitioning of HNO₃, which
51 happens mostly in the daytime. The reaction of OH with NO₂ produces gaseous HNO₃,
52 which subsequently partition into the particle phase. The existence of NH₃ or basic
53 particles enhances this process by NH₃-NH₄⁺ gas-particle equilibrium (Kleeman et al.,
54 2005; Seinfeld and Pandis, 2006); (2) Hydrolysis of N₂O₅, which is more important at
55 nighttime. N₂O₅ forms from the reactions of NO₂, O₃ and NO₃ and hydrolyzes to
56 produce particulate nitrate. They can be summarized as reactions R1-R5 (Brown and
57 Stutz 2012):

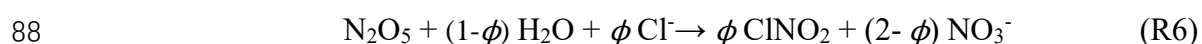


63 In addition to reactions R1 and R5, gas phase reactions of NO₃ with HO₂ and VOCs,
64 N₂O₅ with water vapor (Tuazon et al., 1983) and the heterogeneous reaction of NO₂
65 with water-containing particle (Goodman et al., 1999) produce HNO₃ or nitrate as well.
66 These reactions are listed in Table 2 as reactions R8, R9 and R10.

67 However, chemistry transport models (CTMs) incorporated with these mechanisms

68 still can't accurately capture the spatiotemporal distributions of nitrate in some studies
69 in polluted northern China. For example, Chang et al. (2018) showed that the simulated
70 nitrate concentrations derived from the default CMAQ (version 5.0.2) were
71 significantly higher than the observations in summer at two sites adjacent to Beijing.
72 Fu et al. (2016) also found that default CMAQ (version 5.0.1) overestimated the
73 simulated nitrate concentrations in the Beijing-Tianjin-Hebei region.

74 In recent fields studies, it was found that high particulate chlorine emissions might
75 have a significant impact on the oxidation capacity of the urban atmosphere and thus
76 could affect nitrate concentrations. According to the field measurements in June 2017
77 in Beijing (Zhou et al., 2018), the 2-min averaged concentrations of reactive molecular
78 chlorine (Cl_2) and nitryl chloride (ClNO_2) reached up to 1000 pptv and 1200 pptv,
79 respectively, during some severe air pollution periods in summer. The Cl_2
80 concentrations were significantly higher than those observed in North American coastal
81 cities affected by onshore flow and the lower atmosphere in the remote Arctic region
82 (Spicer et al., 1998; Glasow et al., 2010; Liu et al., 2017). During these pollution events,
83 the corresponding concentrations of N_2O_5 (2-min average) and nitrate (5-min average)
84 rose from 40 pptv and $1 \mu\text{g m}^{-3}$ to 700 pptv and $5 \mu\text{g m}^{-3}$. To explain the high levels of
85 ClNO_2 , some studies suggested that reaction R5 should be revised to account for ClNO_2
86 production from the heterogeneous reaction of N_2O_5 on chloride-containing particles
87 (CPS) (Osthoff et al., 2008; Thornton et al., 2010), as shown in reaction R6:



89 where ϕ represents the molar yield of ClNO_2 . ~~When Cl is enough, this reaction leads~~
90 ~~to lower nitrate concentrations than reaction R5.~~ By incorporating this reaction into
91 WRF-Chem, Li et al. (2016) found that the improved model performed better to match
92 the observed nitrate concentrations in Hongkong during 15 November and 5 December
93 2013. However, ClNO_2 could affect the formation of nitrate indirectly by increasing the
94 atmospheric OH after a series of chemical reactions, which are briefly summarized into
95 three steps: (1) the photolysis of ClNO_2 produces chlorine radicals (Cl^\bullet); (2) the reaction
96 of Cl^\bullet with VOCs produces peroxy radical (HO_2 and RO_2); and (3) the increased HO_2
97 and RO_2 prompt the formation of OH through HOx cycle and lead to increased HNO_3
98 production (Young et al., 2014; Jobson et al., 1994). The overall impact of R6 on nitrate
99 remains to be investigated.

100 Another related but unresolved issue is the sources of the high concentrations Cl_2 ,
101 which could not be explained by the N_2O_5 heterogeneous reaction with Cl^- and the

102 subsequent reactions of ClNO₂ in the gas phase. It has been reported that the reactions
103 of gaseous O₃, OH, HO₂, ClNO₂, hypochlorous acid (HOCl), chlorine nitrate (ClONO₂)
104 with CPS can produce Cl₂, which can subsequently photolyze to produce Cl•
105 (Knipping et al., 2000; George et al., 2010; Pratte et al., 2006; Deiber et al., 2004; Faxon
106 et al., 2015). However, these heterogeneous reactions on CPS are generally missing in
107 most of the current CTMs and it is unclear whether these reactions will be able to
108 explain the observed Cl₂ concentrations and the overall impact of these reactions on
109 nitrate.

110 Previously, biomass burning, coal combustion, and waste incineration were
111 identified as the main sources of gaseous and particulate chlorine compounds in China
112 from International Global Atmospheric Chemistry Program's Global Emissions
113 Inventory Activity (GEIA) based on the year 1990 and a localized study by Fu et al.
114 based on the year 2014 (Keene et al., 1999; Fu et al., 2018). However, recent source
115 apportionment results of PM_{2.5} in Beijing showed that the contribution of coal
116 combustion had extremely decreased from 22.4% in 2014 to 3% in 2017 with the
117 replacement of natural gas (obtained from official website of Beijing Municipal Bureau
118 of Statistics, available at <http://edu.bjstats.gov.cn/>). Another important source—cooking
119 has received attention as its increasing contribution to PM_{2.5} (accounting for 33% of the
120 residential sector; obtained from the official source apportionment analysis of PM_{2.5} in
121 Beijing in 2017; see <http://www.bjepb.gov.cn/bjhr-b/index/index.html>). Moreover, the
122 high content of particulate sodium chloride was measured from the source
123 characterization studies of PM_{2.5} released from the cooking activities (Zhang et al.,
124 2016). Thus, it is necessary to compile an updated emission inventory for Beijing to
125 include the emissions from cooking and other sources (coal burning, solid waste
126 incineration, biomass burning, etc.) in order to explore the emissions of the chlorine
127 species on atmospheric nitrate formation.

128 In this study, a CMAQ model with an improved chlorine heterogeneous chemistry
129 is applied to simulate summer nitrate concentration in Beijing. Sensitivity simulations
130 are conducted to evaluate the contributions of HNO₃ gas-to-particle partitioning and
131 heterogenous production to aerosol nitrate. The results of this work can improve our
132 understandings on nitrate formation and provide useful information on nitrate pollution
133 control strategies in Beijing.

134

135 2. Emissions, chemical reactions and model description

136 2.1 Emissions

137 Generally, the conventional emission inventories of air pollutants in China only include
138 the common chemical species, such as SO₂, NO_x, VOCs, PM_{2.5}, PM₁₀, NH₃, BC, and
139 OC (Wang et al., 2014). Chloride compound emissions were not included. However,
140 the emissions of chlorine species are vital for studying the chlorine chemical
141 mechanism. Recently, the inorganic hydrogen chloride (HCl) and fine particulate
142 chloride (PCL) emission inventories for the sectors of coal combustion, biomass burning,
143 and waste incineration were developed for the year of 2014 (Qiu et al., 2016, Fu et al.,
144 2018, Liu et al., 2018). However, the gaseous chlorine emission was not estimated in
145 these studies. In addition, these studies did not account for the rapid decrease of coal
146 consumption in recent years in Beijing, from 2000 Mt in 2014 to 490 Mt in 2017. More
147 importantly, the cooking source, as one of the major contributors to particulate chlorine
148 in Beijing, is not included in current chlorine emission inventories. Thus, a new
149 emission inventory of reactive chlorine species, which includes HCl, Cl₂ and PCl, were
150 developed in this study for the year of 2017.

151 The emission factor method (equation (1)) is applied to calculate the emissions of
152 these reactive chlorine species from coal combustion, biomass burning, municipal solid
153 waste incineration and industrial processes:

$$154 E_{i,j} = A_i \times EF_{i,j} \quad (1)$$

155 where $E_{i,j}$ represents the emission factor of pollutant j in sector i ; A represents the
156 activity data; EF represents the emission factor. EF for PCl is estimated by $EF_{i,PCL} =$
157 $EF_{i,PM2.5} \times f_{Cl,i}$, where $f_{Cl,i}$ represents the mass fraction of PCl in primary PM_{2.5}.
158 Activity data are obtained from the Beijing Municipal Bureau of Statistics (available at
159 <http://tjj.beijing.gov.cn/>). The Cl₂ emission factor for coal combustion is calculated
160 based on the content of Cl in coal, which had been measured by Deng et al (2017). The
161 PM_{2.5} emission factors and mass fractions of PCl in PM_{2.5} to calculate the emissions of
162 Cl had been described in detail by Fu et al. (2018). PCl in PM_{2.5} for coal combustion
163 and biomass burning are taken as 1% and 9.0%, respectively, based on local
164 measurements in Beijing.

165 Emissions of PCl from cooking, including contributions from commercial and
166 household cooking, are estimated using equation (2):

$$167 E_{PCL} = [N_f \times V_f \times H_f \times EF_{f,PCL} + V_c \times H_c \times N_c \times n \times EF_{c,PCL} \times (1 - \eta)] \times 365 \quad (2)$$

168 where N_f is the number of households, V_f is the volume of exhaust gas from a household
 169 stove ($2000 \text{ m}^3 \text{ h}^{-1}$); H_f is the cooking time for a family (0.5 h day^{-1}); $EF_{f,PCl}$ and
 170 $EF_{c,PCl}$ are the emission factors (kg m^{-3}) of PCl for household and commercial cooking,
 171 respectively; H_c is the cooking time in a commercial cooking facility (6 h day^{-1}); N_c is
 172 the number of restaurants, schools and government departments. V_c is the volume of
 173 exhaust gas from a commercial cooking stove ($8000 \text{ m}^3 \text{ h}^{-1}$); n is the number of stoves
 174 for each unit, which equals to 6 for a restaurant and is calculated as one stove per 150
 175 students for each school. η is the removal efficiency of fume scrubbers (30%). $EF_{c,PCl}$
 176 is the emission factor (kg m^{-3}) of PCl in commercial cooking. These constants are all
 177 based on Wu et al. (2018). The PCl fraction in $\text{PM}_{2.5}$ from cooking is take as 10%, based
 178 on local measurements. HCl and Cl_2 emissions from cooking are not considered in this
 179 study.

180 The sectoral emissions of HCl, Cl_2 and PCl are summarized in Table 1. The
 181 estimated HCl, Cl_2 and PCl emissions in Beijing are 1.89 Gg, 0.07Gg and 0.63Gg
 182 respectively. The Cl emissions estimated for 2014 by Fu et al. (2018) were used for
 183 other areas. This simplification is a good approximation because replacing coal with
 184 natural gas only occurred in Beijing, and reduction of coal consumption in surrounding
 185 regions was generally less than 15%. In addition, strict control measures for biomass
 186 burning, cooking and municipal solid waste incineration have not been implemented in
 187 most regions yet. Emissions of conventional species for this study period are developed
 188 in a separate study that is currently under review and are summarized in Table S1.

189

190 2.2 Chlorine-related heterogeneous reactions

191 The heterogeneous reactions in original CMAQ (version 5.0.1) are not related to
 192 chlorine species. In this study, the original heterogeneous reactions of N_2O_5 and NO_2
 193 (R5 and R10 in Table 2) are replaced with a revised version which includes production
 194 of ClNO_2 from CPS (R6 and R11 in Table 2). In reaction R6, the molar yield of ClNO_2
 195 (ϕ_{ClNO_2}) is represented as equation (3) (Bertram and Thornton, 2009):

$$\phi_{\text{ClNO}_2} = \left(1 + \frac{[\text{H}_2\text{O}]}{483 \times [\text{Cl}^-]} \right)^{-1} \quad (3)$$

196 where $[\text{H}_2\text{O}]$ and $[\text{Cl}^-]$ are the molarities of liquid water and chloride (mol m^{-3}).

197 In addition, laboratory observations confirmed that the heterogeneous uptake of
 198 some oxidants (such as O_3 and OH) and reactive chlorine species (such as ClNO_2 , HOCl ,

199 and ClONO₂) could also occur on CPS to produce Cl₂. These reactions are implemented
 200 in the model and summarized in Table 2 as R13-R18. Note that the products from the
 201 heterogeneous uptake of ClNO₂ on CPS vary with particle acidity (Riedel et al., 2012;
 202 Rossi, 2003). It generates Cl₂ under the condition of pH lower than 2 but produces
 203 nitrate and chloride under higher pH conditions. The reaction rates of the heterogeneous
 204 reactions are parameterized as first-order reactions, with the rate of change of gas phase
 205 species concentrations determined by equations (4) (Ying et al., 2015):

$$\frac{dC}{dt} = -\frac{1}{4}(v\gamma A)C = -k^I C \quad (4)$$

206 where C represents the concentration of species; v represents the thermal velocity of
 207 the gas molecules (m s^{-1}); A is the CMAQ-predicted wet aerosol surface area
 208 concentration ($\text{m}^2 \text{m}^{-3}$); γ represents the uptake coefficient. For all gas phases species
 209 (except ClNO₂) involved in the heterogeneous reactions (R6 and R11-R18), a simple
 210 analytical solution can be used to update their concentrations from time t_0 to $t_0+\Delta t$:
 211 $[C]_{t_0+\Delta t}=[C]_{t_0} \exp(-k^I \Delta t)$, where Δt is the operator-splitting time step for heterogeneous
 212 reactions.

213 The rate of change of ClNO₂ includes both removal and production terms, as shown
 214 in equation (5):

$$\begin{aligned} \frac{d[\text{ClNO}_2]}{dt} &= -k_i^I [\text{ClNO}_2] + k_6^I \phi_{\text{ClNO}_2} [\text{N}_2\text{O}_5] \\ &= -k_i^I [\text{ClNO}_2] + k_6^I \phi_{\text{ClNO}_2} [\text{N}_2\text{O}_5]_{t_0} \exp(-k_6^I t) \end{aligned} \quad (5)$$

215 Assuming ϕ_{ClNO_2} is a constant, an analytical solution for equation (5) can be obtained,
 216 as shown in equation (6):

$$\begin{aligned} [\text{ClNO}_2]_{t_0+\Delta t} &= [\text{ClNO}_2]_{t_0} \exp(-k_i^I \Delta t) \\ &+ \frac{k_6^I \phi_{\text{ClNO}_2} [\text{N}_2\text{O}_5]_{t_0}}{k_i^I - k_6^I} [\exp(-k_6^I \Delta t) - \exp(-k_i^I \Delta t)] \end{aligned} \quad (6)$$

217 where k_i^I represents the pseudo first-order rate coefficient of either reaction R17 or
 218 R18, depending on pH.

219 The uptake coefficients γ of gaseous species are obtained from published
 220 laboratorial studies. In the original CMAQ, the uptake coefficient of N₂O₅ is determined
 221 as a function of the concentrations of (NH₄)₂SO₄, NH₄HSO₄ and NH₄NO₃ (Davis et al.,
 222 2008). In this study, the PCl and NO₃⁻ dependent parameterization by Bertram and
 223 Thornton (2009) (equation (7)) is used:

$$\gamma_{N_2O_5} = \begin{cases} 0.02, & \text{for frozen aerosols} \\ 3.2 \times 10^{-8} K_f \left[1 - \left(1 + \frac{6 \times 10^{-2} [H_2O]}{[NO_3^-]} + \frac{29 [Cl^-]}{[NO_3^-]} \right)^{-1} \right] & \end{cases} \quad (7)$$

224 In the above equation, K_f is parameterized function based on molarity of water: $K_f =$
 225 $1.15 \times 10^6 (1 - e^{-0.13[H_2O]})$. NO_3^- and Cl^- concentrations are also in molarity. The
 226 uptake coefficient of OH is expressed in equation (8) as a function of the concentration
 227 of PCI following the IUPAC (International Union of Pure and Applied Chemistry,
 228 available at [http://iupac.poleether.fr/htdocs/datasheets/pdf/O-](http://iupac.poleether.fr/htdocs/datasheets/pdf/O-H_halide_solutions_VI.A2.1.pdf)
 229 [H_halide_solutions_VI.A2.1.pdf](http://iupac.poleether.fr/htdocs/datasheets/pdf/O-H_halide_solutions_VI.A2.1.pdf)).

$$\gamma = \gamma_{OH} = \min\left(0.04 \times \frac{[Cl^-]}{1000 \times M}, 1\right) \quad (8)$$

230 where M represents the volume of liquid water in aerosol volume ($m^3 m^{-3}$). For frozen
 231 particles, the uptake coefficient is limited to 0.02, as used in the original CMAQ model.

232 The uptake coefficients of O_3 , NO_3 , NO_2 , $HOCl$, $ClONO_2$, and $ClONO_2$ are treated
 233 as constants. Among of them, the γ values of NO_3 , NO_2 , $HOCl$ and $ClONO_2$ are set as
 234 3×10^{-3} , 1×10^{-4} , 1.09×10^{-3} and 0.16 based on laboratory measurements (Rudich et al.,
 235 1996; Abbatt et al., 1998; Pratte et al., 2006; Gebel et al., 2001). A preliminary value
 236 of 10^{-3} in the daytime and 10^{-5} at nighttime is chosen for the O_3 uptake coefficient. The
 237 daytime γ_{O_3} is based on the analysis of Cl_2 production rate in a hypothesized
 238 geochemical cycle of reactive inorganic chlorine in the marine boundary layer by Keene
 239 et al. (1990). The lower nighttime value was also recommended by Keene et al. (1990)
 240 who noted that Cl_2 production in the marine boundary layer are lower at night. The
 241 uptake coefficient of $ClONO_2$ depends on the particle acidity, with the value of 2.65×10^{-6}
 242 for reaction R17 and 6×10^{-3} for reaction R18 (Robert et al., 2008).

243

244 2.4 CMAQ model configuration

245 These heterogeneous reactions of chlorine are incorporated into a revised CMAQ based
 246 on the CMAQ version 5.0.1 to simulate the distribution of nitrate concentration in
 247 Beijing from 11 to 15 June 2017. The revised CMAQ model without heterogeneous
 248 reactions of chlorine has been described in detail by Ying et al. (2015) and Hu et al.
 249 (2016, 2017). In summary, the gas phase chemical mechanism in the revised CMAQ
 250 model is based on the SAPRC-11 (Cater et al., 2012) with a comprehensive inorganic
 251 chlorine chemistry. Reactions of Cl radical with several major VOCs, which lead to

252 production of HCl, are also included. The aerosol module is based on AERO6 with an
253 updated treatment of NO₂ and SO₂ heterogeneous reaction and formation of secondary
254 organic aerosol from isoprene epoxides. Three-level nested domains with the
255 resolutions of 36km, 12km, and 4km using Lambert Conformal Conic projection
256 (173×136, 135×228 and 60×66 grid cells) are chosen in this work (the domains see
257 Figure S1). The two true latitudes are set to 25°N and 40°N and the origin of the domain
258 is set at 34°N, 110°E. The left-bottom coordinates of the outmost domain are positioned
259 at x = -3114 km, y = -2448 km. The BASE case (heterogeneous reactions of Cl turned
260 off) and HET case (all heterogeneous reactions enabled) are compared to evaluate the
261 impact of heterogeneous chlorine chemistry on nitrate formation.

262

263 **3. Results**

264 3.1 Model performance evaluation

265 Predicted O₃, NO₂ and PM_{2.5} concentrations from the BASE case simulation are
266 evaluated against monitoring data at 12 sites in Beijing (Table S2) in 11 to 15, June
267 2017. The average NMB/NME values for O₃, NO₂ and PM_{2.5} across the 12 sites are -
268 8%/29%, -7%/59% and -8%/53%, respectively. Predicted hourly Cl₂, ClNO₂ and N₂O₅
269 concentrations were compared with observations measured at the Institute of
270 Atmospheric Physics (IAP), Chinese Academy of Sciences (39.98°N, 116.37°E) using
271 a high-resolution time-of-flight chemical ionization mass spectrometer (CIMS) from 11
272 to 15 June 2017 (for site description, instrument introduction, and analytical method,
273 please refer to the study by Zhou et al. (2018)). Figure 1 shows that the concentrations
274 of Cl₂ and ClNO₂ in BASE case are rather low (close to 0), proving that the gas-phase
275 chemistry is not the major pathway to produce Cl₂ and ClNO₂. By contrast, the
276 simulated Cl₂ and ClNO₂ concentrations in HET case increase significantly,
277 correspondingly the NMB and NME changes from -100% to -54% and 100% to 61%
278 for Cl₂, and from -100% to -58% and 100% to 62% for ClNO₂, respectively (the particle
279 surface area concentrations is scaled up by a factor of 5 in daytime and 10 in nighttime
280 because this parameter is underestimated compared to the measured concentrations
281 reported by Zhou et al. (2018)). The simulations of Cl₂ and ClNO₂ are improved as the
282 additional heterogeneous reactions prompt the production of gas phase molecular
283 chlorine. Overall, however, the Cl₂ and ClNO₂ concentrations are still underestimated.
284 Both BASE and HET simulations generally capture the hourly N₂O₅ concentrations as

285 well as the peak values (Figure 1(c)) with similar overall NMB and NME values.

286 The uptake coefficient of O_3 could be an important factor affecting the predicted
287 Cl_2 concentrations as it is found that the heterogeneous reaction of O_3 is the major
288 source of Cl_2 during this period (see discussion in Section 3.2). The influence of
289 different parametrizations of the uptake coefficient of N_2O_5 on $ClNO_2$ and nitrate
290 concentrations are also discussed in Section 3.2.

291 Predicted NO_3^- and PCl concentrations are compared with observations measured
292 at an adjacent monitoring site located at the rooftop of School of Environment building
293 in Tsinghua University (THU, 40.00°N, 116.34°E, about 5 km from IAP) using an
294 Online Analyser of Monitoring of Aerosol and Gases (MARGA) from 11 to 15 June
295 2017. According to Figure 1(d), the simulated nitrate concentration is slightly lower
296 than the observations most of the time. From the evening hours of 12 June to morning
297 hours of 13 June, observed and simulated nitrate concentration both increase
298 significantly. The NMB and NME values of hourly nitrate for the HET case (-5% and
299 39%, respectively) are slightly lower than those for the BASE case -10% and 46%)
300 during this high concentration period. The HET case also generally captures the day-
301 to-day variation of PCl concentration and perform better than the BASE case,
302 correspondingly the NMB and NME are reduced from -48% and 72% to -37% and 67%.
303 The substantial underestimation of PCl in the daytime on 15 June is likely caused by
304 missing local emissions during this period.

305

306 3.2 Impact of uptake coefficients of O_3 and N_2O_5 on chlorine species and nitrate

307 The uptake coefficients of O_3 and N_2O_5 may be important factors affecting the accuracy
308 of simulated nitrate concentrations. Some studies have confirmed that the reaction of
309 O_3 on CPS can indirectly affect the nitrate formation by increasing the atmospheric Cl_2
310 and OH level (Li et al., 2016; Liu et al., 2018). According to Figure 1(a), the improved
311 model still substantially underestimates the concentration of Cl_2 , which may be
312 associated with the underestimation of the uptake coefficients of O_3 , which are
313 empirical and have not been confirmed by laboratory studies. The uptake coefficients
314 were increased by a factor of 10 (0.01 for daytime and 10^{-4} for nighttime) to evaluate
315 the sensitivity of Cl_2 production and nitrate formation to this parameter. Figure 2 shows
316 that the simulated Cl_2 and nitrate concentrations in daytime increase significantly
317 (especially for Cl_2) and sometimes can capture the peak value (such as the daytime peak
318 on 14 June). However, although the NMB and NME of Cl_2 and nitrate improve from -

319 18% and 39% to 1% and 28% when the new uptake coefficients are used, the simulated
320 Cl₂ concentrations are still quite different from the observations (such as during the
321 daytime in 11 and 12 June, see Figure 2). A non-constant parameterization of the uptake
322 coefficients of O₃ that considers the influence of PCl concentrations, meteorology
323 conditions, etc., similar to those of OH and N₂O₅, might be needed. Further laboratory
324 studies should be conducted to provide a better estimation of this important parameter.

325 Several parameterizations for the uptake coefficient of N₂O₅ have been developed
326 for regional and global models and have been evaluated in several previous studies
327 (Tham et al., 2019, 2018, McDuffie et al., 2018a, 2018b). In addition to the
328 parameterization of Bertram and Thornton (2009) used in the HET case, two additional
329 simulations were performed to assess the impact of the uptake coefficient of N₂O₅ on
330 nitrate formation. The first simulation uses the original CMAQ parameterization of
331 Davis et al. (2008) and second simulation uses a constant value of 0.09, which is the
332 upper limit of the N₂O₅ uptake coefficient derived by Zhou et al. (2018) based on
333 observations. The results from the simulations with the parameterization of Bertram
334 and Thornton (2009) generally agree with the results using those based on Davis et al.
335 (2008) ~~and the~~. The application of larger constant and fixed N₂O₅ uptake coefficient
336 leads to slightly better results, which might reflect the fact that the N₂O₅ concentrations
337 are underestimated. Using the uptake coefficient of 0.09 can generally increase the
338 concentration of nitrate in some periods, but it also leads to significant increase of the
339 nitrate level (such as nighttime on 12-13 June and 13-14 June), which is 4-6 times
340 higher than those based on Bertram and Thornton (2009). Overall, predicted nitrate
341 concentrations are sensitive to changes in the changes in $\gamma_{N_2O_5}$, with approximately 50%
342 increase in the nitrate when a constant of $\gamma_{N_2O_5}$ of 0.09 is used.

343

344 3.3 Spatial distributions of nitrate and chlorine species concentrations

345 The regional distributions of averaged Cl₂, ClNO₂, N₂O₅ and NO₃⁻ concentration from
346 11 to 15 June for the HET case are shown in Figure 3. Compared to the BASE case, the
347 episode average concentrations of Cl₂ and ClNO₂ from the HET case increase
348 significantly in the eastern region of Beijing, reaching up to 23 ppt and 71 ppt from near
349 zero (Figure 3a and 3b). High concentrations are not found in the southern region with
350 intensive emissions of chlorine species (Figure S2). The production of ClNO₂ requires
351 the presence of chloride, NO₂, and O₃. In the areas close to the fresh emissions, O₃ is

352 generally low (Figure S3), and the production of NO_3 (hence N_2O_5 and ClNO_2) is
353 limited. Therefore, the production rate of ClNO_2 is generally low in areas affected by
354 fresh emissions. Since the contribution of direct emissions to Cl_2 is low and it is
355 predominantly produced secondarily in the atmosphere, high levels of Cl_2 are also
356 found away from the fresh emissions.

357 The spatial distribution of N_2O_5 concentrations differs from that of other species
358 (Figure 3c). While the concentrations of most of the species are higher in the southern
359 region, the N_2O_5 concentrations are lower in some parts of this region. This is because
360 the O_3 concentration in the core urban areas is low due to high NO_x emissions. The
361 N_2O_5 concentrations from the HET case are approximately 16% lower on average
362 (Figure 3d) because the Bertram and Thornton (2009) parameterization used in the HET
363 case generally gives higher uptake coefficients than the parameterization of Davis et al.
364 (2008) used in the BASE case (Table 3).

365 Although the higher uptake coefficients of N_2O_5 in the HET case facilitate faster
366 conversion of N_2O_5 to nitrate, the nitrate concentrations do not always increase. During
367 daytime hours, nitrate concentrations in the HET case increase due to higher OH (Figure
368 3e and Figure 3f), [increased OH see Figure S4](#)). At nighttime, in contrast, the nitrate
369 concentration decreases significantly in some regions by about 22%, mainly due to
370 lower molar yield of nitrate from the N_2O_5 heterogeneous reaction in the HET case
371 (Figure 3g and Figure 3h). Although ClNO_2 produced in the N_2O_5 reaction also
372 produces nitrate through a heterogeneous reaction when the particle pH is above 2, which
373 is true for most regions (see Figure [S4S5](#)), the uptake coefficient of ClNO_2 is
374 significantly lower than that of N_2O_5 ($0.01\sim 0.09$ for N_2O_5 and 6×10^{-3} for ClNO_2),
375 leading to an overall decrease of nitrate production. As the ClNO_2 production from the
376 heterogeneous reaction leads to less N_2O_5 conversion to non-relative nitrate, it may
377 change the overall lifetime of NO_x and their transport distances. The magnitude of this
378 change and its implications on ozone and $\text{PM}_{2.5}$ in local and downwind areas should be
379 further studied.

380

381 3.4 Relationship between nitrate formation and chlorine chemistry

382 Nitrate productions from the homogeneous and heterogeneous pathways in Beijing are
383 approximated by the difference in predicted nitrate concentrations between the BASE
384 or HET case and a sensitivity case without heterogeneous reactions. Averaging over the
385 five-day period, approximately 58% of the nitrate originates from HNO_3 gas-to-particle

386 partitioning and 42% is from heterogeneous reactions (Figure 4). This conclusion
387 generally agrees with measurements at Peking University (PKU) (52% from the
388 heterogeneous process and 48% from HNO₃ partitioning) on four polluted days
389 (average in September 2016 reported by Wang et al. (2017)). Slightly higher
390 contributions of the homogeneous pathway in this study is expected because of high
391 OH concentrations during the day and lower particle surface areas at night.

392 The nitrate formation from different homogeneous and heterogeneous pathways in
393 the BASE case and HET case are further studied. Contributions of different gas phase
394 pathways are determined using the process analysis tool in CMAQ. Contributions of
395 different heterogeneous pathways are determined using a zero-out method that turns off
396 one heterogeneous pathway at a time in a series of sensitivity simulations. Figure 4
397 shows that the reaction of OH and NO₂ is always the major pathway for the formation
398 of nitrate through homogeneous formation of HNO₃ and gas-to-particle partitioning.
399 However, its nitrate production rate through this homogeneous pathway decreases
400 significantly from daytime to nighttime (from 1.81 μg m⁻³ h⁻¹ to 0.33 μg m⁻³ h⁻¹ on
401 average). The nitrate production from other HNO₃ partitioning pathways in the daytime
402 is negligible. At nighttime, homogeneous reaction of N₂O₅ with water vapor accounts
403 for approximately 5% of the overall homogeneous nitrate formation. For the
404 heterogeneous pathways, daytime production rate is approximately 0.6 μg m⁻³ h⁻¹ with
405 1/3 of the contributions from NO₂ and 2/3 from N₂O₅. Nighttime production on nitrate
406 from the heterogeneous pathways is approximately 3.1 μg m⁻³ h⁻¹, of which 85% is due
407 to N₂O₅ and 15% is due to NO₂.

408 Comparing the BASE case and the HET case shows that, when the chlorine
409 chemistry is included, the gaseous HNO₃ produced by OH reacting with NO₂ increases
410 significantly in the HET case. Correspondingly, the nitrate production rate reaches up
411 to 2.04 μg m⁻³ h⁻¹ in the daytime due to increased atmospheric OH concentrations
412 predicted by the chlorine reactions. Similar conclusions are also obtained by Li et al.
413 (2016) and Liu et al. (2017) based on observations and model simulations. The
414 heterogeneous production of nitrate from the reaction of N₂O₅ uptake decreases by
415 approximately 27% in the HET case due to the production of gas phase ClNO₂.
416 According to the study by Sarwar et al. (2012; 2014), including the heterogeneous
417 reaction of N₂O₅ with PCl decreased the nocturnal nitrate concentration by 11-21% in
418 the United States, which was slightly less than the current study for Beijing. It is likely
419 because PCl concentrations in the United States are significantly lower than those in

420 Beijing (the monthly PCl concentration is $0.06 \mu\text{g m}^{-3}$ in the United State against $\sim 1 \mu\text{g}$
421 m^{-3} in Beijing) so that PCl is depleted quickly. The contributions of NO_2 uptake to
422 nitrate also decrease by 22% because of the lower rate constant of the reaction of NO_2
423 with PCl. In contrast, the contribution of ClNO_2 reacts with particle surface to nitrate
424 production increases by 6% in the HET case. The overall nitrate concentration in the
425 HET case is about 22% higher than that in the BASE case during this study period.

426

427 **4. Conclusions**

428 In this work, a modified CMAQ model incorporated with heterogeneous reactions for
429 the production of molecular chlorine and other reactive chlorine species is developed
430 and its impact on of the nitrate formation predictions are evaluated. The contributions
431 from different homogenous and heterogeneous pathways to nitrate formation are also
432 quantified. High concentration of Cl_2 and ClNO_2 do not occur in the southern part of
433 the Beijing-Tianjin-Hebei region with intensive emissions of chlorine species as higher
434 concentrations of O_3 and N_2O_5 associated with the heterogeneous formation of these
435 species generally occurred in the downwind areas. CTMs without a complete treatment
436 of the chlorine chemistry can underestimate daytime nitrate formation from the
437 homogeneous pathways, particularly from HNO_3 gas-to-particle partitioning due to
438 underestimation of OH concentrations and overestimate the nighttime nitrate formation
439 from the heterogeneous pathways due to missing chlorine heterogeneous chemistry.

440

441 **Data availability.** The data in this study are available from the authors upon request
442 (shxwang@tsinghua.edu.cn)

443

444 **Author contributions.** XQ, QY, SW and JH designed the study; YS, BL, AS, XY
445 provided observation data; XQ, QY, SW, JZ, QX, DD, LD and JX analyzed data. XQ,
446 QY and SW wrote the paper.

447

448 **Competing interests.** The authors declare that they have no conflict of interest.

449

450 **Acknowledgments.** This work was supported by National Natural Science Foundation
451 of China (21625701), China Postdoctoral Science Foundation (2018M641385),
452 National Research Program for Key Issue in Air Pollution Control (DQGG0301,
453 DQGG0501) and National Key R&D Program of China (2018YFC0213805,

454 2018YFC0214006). The simulations were completed on the “Explorer 100” cluster
455 system of Tsinghua National Laboratory for Information Science and Technology.

- 457 Abbatt, J. P., Waschewsky, G. C., et al.: Heterogeneous interactions of HOBr, HNO₃, O₃, and NO₂
458 with deliquescent NaCl aerosols at room temperature. *J. Phys. Chem, A.*, 102, 3719-3725, 1998.
- 459 Bertram, T. H., Thornton, J. A.: Toward a general parameterization of N₂O₅ reactivity on aqueous
460 particles: the competing effects of particle liquid water, nitrate and chloride. *Atmos. Chem.*
461 *Phys.*, 9, 8351-8363, 2009.
- 462 Brown, S.S., Stutz, J. Nighttime radical observations and chemistry. *Chemical Society Reviews*, 41,
463 6405-6447, 2012.
- 464 Cater, W. P. L., Heo, G.: Development of revised SAPRC aromatics mechanisms. Final Report to
465 the California Air Resources Board, Contracts No. 07-730 and 08-326, April 12, 2012
- 466 Chang, X., Wang, S., Zhao, B., et al.: Assessment of inter-city transport of particulate matter in the
467 Beijing–Tianjin–Hebei region, *Atmos. Chem. Phys.*, 18, 4843-4858,
468 <https://doi.org/10.5194/acp-18-4843-2018>, 2018.
- 469 Davis, J. M., Bhawe, P. V., Foley, K. M.: Parameterization of N₂O₅ reaction probabilities on the
470 surface of particles containing ammonium, sulfate, and nitrate. *Atmos. Chem. Phys.* 8, 5295-
471 5311, 2008.
- 472 Deng, S., Zhang, C., Liu, Y., et al.: A Full-Scale Field Study on Chlorine Emission of Pulverized
473 Coal-Fired Power Plants in China. *Research of Environmental Science*. In Chinese, 27, 127-
474 133, 2014.
- 475 Deiber, G., George, C., Le Calve, S., Schweitzer, F., Mirabel, P.: Uptake study of ClONO₂ and
476 BrONO₂ by Halide containing droplets. *Atmos. Chem. Phys.* 4, 1291-1299, 2004.
- 477 Ding, D.; Xing, J.; Wang, S. X.; et al.: Emission reductions dominate the decline in the ambient
478 PM_{2.5} concentration and related mortality during 2013-2017 in China. *Environ. Health*
479 *Perspect.*, under review.
- 480 Faxon, C. B., Bean, J. K., Hildebrandt R.L.: Inland Concentrations of Cl₂ and ClONO₂ in Southeast
481 Texas Suggest Chlorine Chemistry Significantly Contributes to Atmospheric Reactivity.
482 *Atmosphere*, 6, 1487-1506, 2015.
- 483 Fu, X., Wang, S.X., Chang, X., et al.: Modeling analysis of secondary inorganic aerosols over China:
484 pollution characteristics, and meteorological and dust impacts. *Sci. Rep.* 6, 35992, 2016.
- 485 Fu, X., Wang, T., Wang, S. X., et al.: Anthropogenic Emissions of Hydrogen Chloride and Fine
486 Particulate Chloride in China. *Environ. Sci. Technol.* 52, 1644-1654, 2018.
- 487 George, I. J., Abbatt, J. P.: Heterogeneous oxidation of atmospheric aerosol particles by gas-phase
488 radicals. *Nat. Chem.* 2, 713-722, 2010.
- 489 Gebel, M. E., Finlayson-Pitts, B. J.: Uptake and reaction of ClONO₂ on NaCl and synthetic sea salt.
490 *J. Phys. Chem. A*, 105, 5178-5187, 2001.
- 491 Glasow, V.R. Wider role for airborne chlorine. *Nature*. 464, 168-169. 2010.
- 492 Goodman, A.L., Underwood, G.M., Grassian, V.H.: Heterogeneous reaction of NO₂:
493 characterization of gas-phase and adsorbed products from the reaction, 2NO₂(g) + H₂O(a) →
494 HONO(g) + HNO₃(a) on Hydrated Silica Particles. *The Journal of Physical Chemistry A* 103,
495 7217-7223, 1999.
- 496 Hu, J., Chen, J., Ying, Q., Zhang, H.: One-Year Simulation of Ozone and Particulate Matter in China
497 Using WRF/CMAQ Modeling System. *Atmos. Chem. Phys.* 16, 10333-10350, 2016.
- 498 Hu, J., Wang, P., Ying, Q., Zhang, H., Chen, J., Ge, X., Li, X., Jiang, J., Wang, S., Zhang, J., Zhao,
499 Y., Zhang, Y.: Modeling biogenic and anthropogenic secondary organic aerosol in China.
500 *Atmos. Chem. Phys.* 17, 77-92, 2017.
- 501 Jobson, B. T., Niki, H., Yokouchi, Y., et al.: Measurements of C2-C6 hydrocarbons during the Polar
502 Sunrise 1992 experiment: Evidence for Cl atom and Br atom chemistry, *J. Geophys. Res.*, 99,
503 25355-25368, 1994.
- 504 Keene, W. C.; Pszenny, A. A. P.; Jacob, D. J.; Duce, R. A.; Galloway, J. N.; Schultz-Tokos, J. J.;
505 Sievering, H.; Boatman, J. F.: The Geochemical Cycling of Reactive Chlorine through the
506 Marine Troposphere. *Global. Biogeochem.*, 4, 407-430, 1990.
- 507 Keene, W. C., Khalil, M. A. K., Erickson, D. J., et al.: Composite global emissions of reactive
508 chlorine from anthropogenic and natural sources: Reactive Chlorine Emissions Inventory. *J.*
509 *Geophys. Res-Atmos.*, 104, 8429-8440, 1999.
- 510 Kleeman, M.J., Ying, Q., Kaduwela, A.: Control strategies for the reduction of airborne particulate
511 nitrate in California's San Joaquin Valley. *Atmos. Environ.*, 39, 5325-5341, 2005.
- 512 Knipping, E. M., Lakin, M. J., Foster, K. L., Jungwirth, P., Tobias, D. J., Gerber, R. B., Dabdub, D.,

513 Finlayson-Pitts, B. J.: Experiments and simulations of ion-enhanced interfacial chemistry on
514 aqueous NaCl aerosols. *Science*, 288, 301-306, 2000.

515 Li, H.Y., Zhang, Q., Zheng, B., et al.: Nitrate-driven urban haze pollution during summertime over
516 the North China Plain. *Atmos. Chem. Phys.*, 18, 5293-5306, 2018.

517 Li, Q.Y., Zhang, L., Wang, T., et al. Impacts of heterogeneous uptake of dinitrogen pentoxide and
518 chlorine activation on ozone and reactive nitrogen partitioning: improvement and application
519 of the WRF-Chem model in southern China. *Atmos. Chem. Phys.*, 16, 14875-14890, 2016.

520 Liu, X. X., Qu, H., Huey, L. G., et al.: High Levels of Daytime Molecular Chlorine and Nitryl
521 Chloride at a Rural Site on the North China Plain. *Environ. Sci. Technol.*, 51, 9588-9595, 2017.

522 Liu, Y.M., Fan, Q., Chen, X.Y.: Modeling the impact of chlorine emissions from coal combustion
523 and prescribed waste incineration on tropospheric ozone formation in China. *Atmos. Chem.*
524 *Phys.*, 18, 2709-2724, 2018.

525 Ma, X.Y., Sha, T., Wang, J.Y., et al.: Investigating impact of emission inventories on PM_{2.5}
526 simulations over North China Plain by WRF-Chem. *Atmos. Environ.*, 195, 125-140. 2018.

527 McDuffie, E.E., Fibiger, D.L., Dubé, W.P., et al.: Heterogeneous N₂O₅ uptake during winter: Aircraft
528 measurements during the 2015 WINTER campaign and critical evaluation of current
529 parameterizations. *J. Geophys. Res.: Atmos.*, 123, 4345-4372, 2018a.

530 McDuffie, E.E., Fibiger, D.L., Dubé, W.P., et al.: ClNO₂ yields from aircraft measurements during
531 the 2015 WINTER campaign and critical evaluation of the current parameterization. *J.*
532 *Geophys. Res. Atmos.*, 123, 12-994, 2018b.

533 Osthoff, H.D., Roberts, J.M., Ravishankara, A.R.: High levels of nitryl chloride in the polluted
534 subtropical marine boundary layer. *Nat. Geosci.*, 1, 324-328, 2008.

535 Pratte, P., Rossi, M. J.: The heterogeneous kinetics of HOBr and HOCl on acidified sea salt and
536 model aerosol at 40-90% relative humidity and ambient temperature. *Phys. Chem. Chem. Phys.*
537 8, 3988-4001, 2006.

538 Qiu, X.H., Chai, F.H., Duan, Lei., et al.: Deriving High-Resolution Emission Inventory of Open
539 Biomass Burning in China based on Satellite Observations. *Environ. Sci. Technol.*, 50, 11779-
540 11786, 2016.

541 Riedel, T. P.; Bertram, T. H.; Crisp, T. A.; Williams, E. J.; Lerner, B. M.; Vlasenko, A.; Li, S. M.;
542 Gilman, J.; de Gouw, J.; Bon, D. M.; Wagner, N. L.; Brown, S. S.; Thornton, J. A., Nitryl
543 Chloride and Molecular Chlorine in the Coastal Marine Boundary Layer. *Environ Sci Technol.*,
544 46, 10463-10470, 2012.

545 Roberts, J. M., Osthoff, H. D., Brown, S. S., et al.: N₂O₅ oxidizes chloride to Cl₂ in acidic
546 atmospheric aerosol. *Science*, 321, 1059-1059, 2008.

547 Song, S.J., Gao, M., Xu, W.Q., et al.: Fine-particle pH for Beijing winter haze as inferred from
548 different thermodynamic equilibrium models. *Atmos. Chem. Phys.*, 18, 7423-7438, 2018.

549 Rossi, M J. Heterogeneous Reactions on Salts. *Chemical Reviews*, 103, 4823-4882, 2003.

550 Rudich, Y., Talukdar, R.K., Ravishankara, A.R., et al.: Reactive uptake of NO₃ on pure water and
551 ionic solutions. *J. Geophys. Res.* 101, 21023-21031, 1996.

552 Sarwar, G., Simon, H., Bhave, P.: Examining the impact of heterogeneous nitryl chloride production
553 on air quality across the United States. *Atmospheric Chemistry and Physics*, 12, 6455-6473,
554 2012.

555 Sarwar, G., Simon, H., Xing, J: Importance of tropospheric ClNO₂ chemistry across the Northern
556 Hemisphere. *Geophysical Research Letters*, 41, 4050-4058, 2014.

557 Seinfeld, J.H., Pandis, S.N.: *Atmospheric Chemistry and Physics: From Air Pollution to Climate*
558 *Change*. Wiley-Interscience, New York. 2006.

559 Song, S. J., Gao, M., Xu, W. Q.: Fine-particle pH for Beijing winter haze as inferred from different
560 thermodynamic equilibrium models. *Atmos. Chem. Phys.*, 18, 7423-7438, 2018.

561 Spicer, C.W., Chapman, E.G., Finlayson-Pitts., et al.: Unexpectedly high concentrations of
562 molecular chlorine in coastal air. *Nature*, 394, 353-356, 1998.

563 Thornton, J.A., Kercher, J.P., Riedel, T.P., et al.: A large atomic chlorine source inferred from mid-
564 continental reactive nitrogen chemistry. *Nature*, 464, 271-274, 2010.

565 Tham, Y.J., Wang, Z., Li, Q., et al.: Heterogeneous N₂O₅ uptake coefficient and production yield of
566 ClNO₂ in polluted northern China: roles of aerosol water content and chemical composition.
567 *Atmospheric Chemistry and Physics*, 18, 13155-13171, 2018.

568 Tuazon, E.C., Atkinson, R., Plum, C.N., Winer, A.M., Pitts Jr., J.N.: The reaction of gas phase N₂O₅
569 with water vapor. *Geophysical Research Letters* 10, 953-956, 1983.

570 Wang, S.X., Zhao, B., Cai, S.Y., et al.: Emission trends and mitigation options for air pollutants in
571 East Asia. *Atmos. Chem. Phys.*, 14, 6571-6603, 2014.

572 Wang, H.C., Lu, K.D., Chen, X.R., et al.: High N₂O₅ concentrations observed in urban Beijing:
573 implications of a large nitrate formation pathway. *Environ. Sci. Technol. Lett.* 4, 416-420, 2017.

574 Wen, L., Xue, L.K., Wang, X.F., et al.: Summertime fine particulate nitrate pollution in the North
575 China Plain: increasing trends, formation mechanisms and implications for control policy.
576 *Atmos. Chem. Phys.*, 18, 11261-11275, 2018.

577 Wu, X.W., Chen, W.W., Wang, K., et al.: PM_{2.5} and VOCs emission inventories from cooking in
578 Changchun city. *China Environmental Science*, 38, 2882-2889, 2018.

579 Ying, Q., Li, J. Y., Kota, S. H.: Significant Contributions of Isoprene to Summertime Secondary
580 Organic Aerosol in Eastern United States. *Environ. Sci. Technol.*, 49, 7834-7842, 2015.

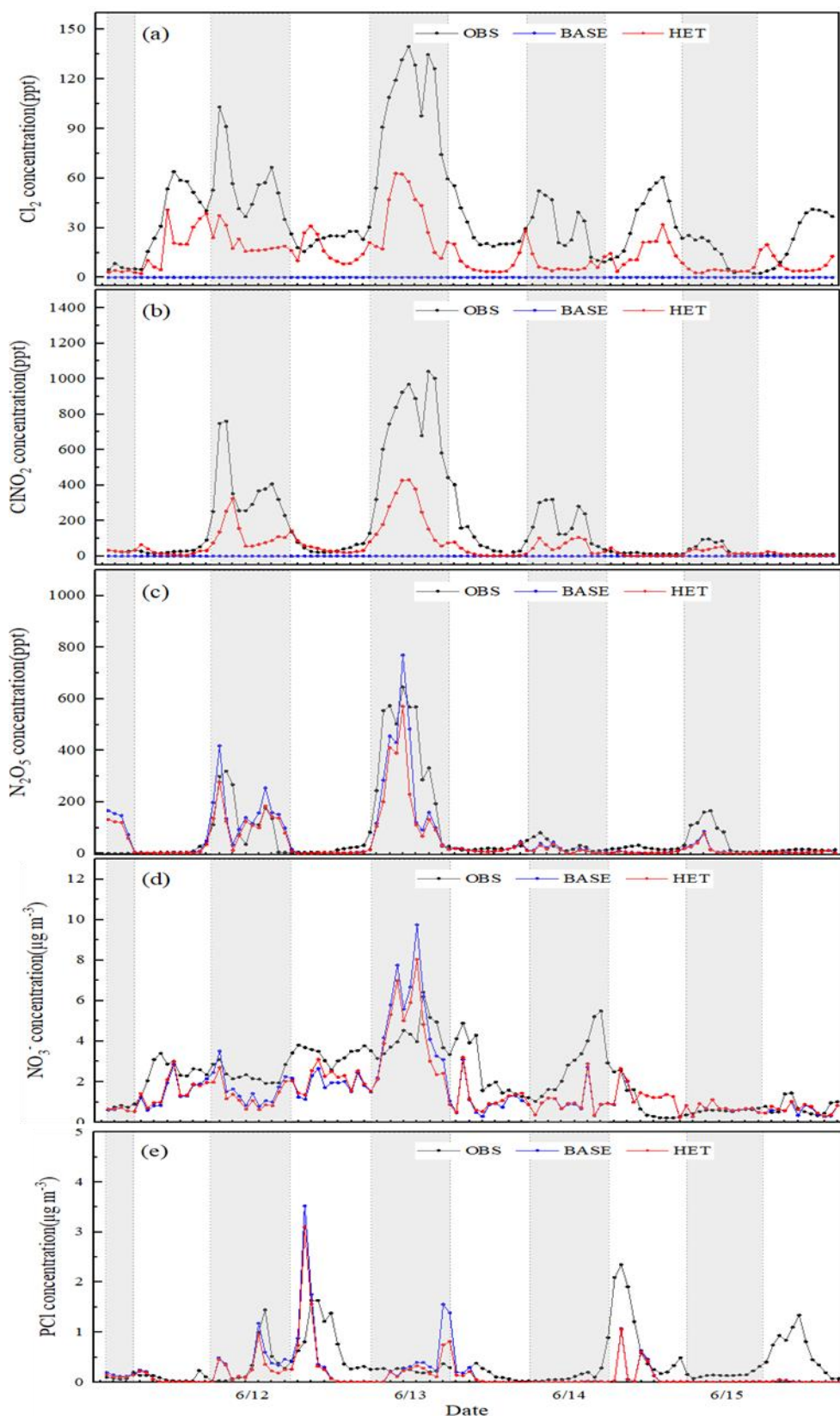
581 Young, C.J., Washenfelder, R.A., Edwards, P.M., et al.: Chlorine as a primary radical: evaluation of
582 methods to understand its role in the initiation of oxidative cycles. *Atmos. Chem. Phys.* 14,
583 3247-3440, 2014.

584 Zhang, T., Peng, L., Li, Y.H.: Chemical characteristics of PM_{2.5} emitted from cooking fumes. *Res.*
585 *Environ. Sci.*, 29, 183-191, 2016. In Chinese.

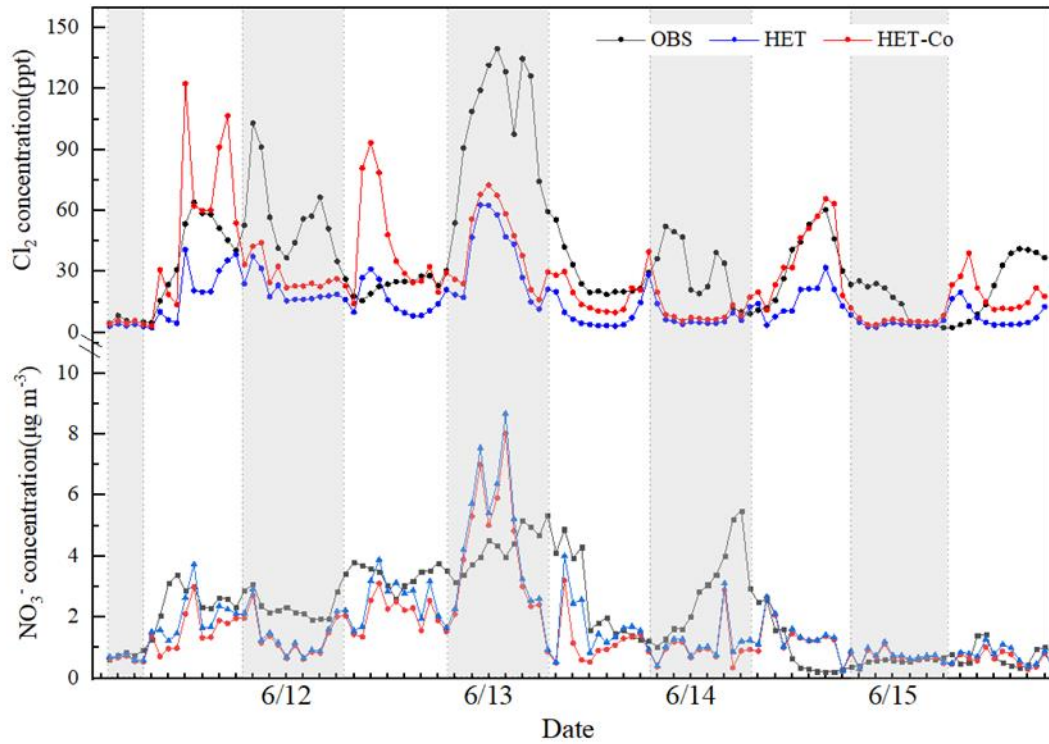
586 Zhou, W., Zhao, J., Ouyang, B., et al.: Production of N₂O₅ and ClNO₂ in summer in urban Beijing,
587 China., *Atmos. Chem. Phys.*, 18,11581-11597, 2018.

588

589



590
 591 Figure 1 Comparison of observed hourly Cl_2 , ClNO_2 , N_2O_5 (at the Institute of
 592 Atmospheric Physics, Chinese Academy of Sciences), NO_3^- and PCl (at Tsinghua
 593 University) in urban Beijing with predictions from the BASE and the HET cases
 594 during 11-15 June 2017.



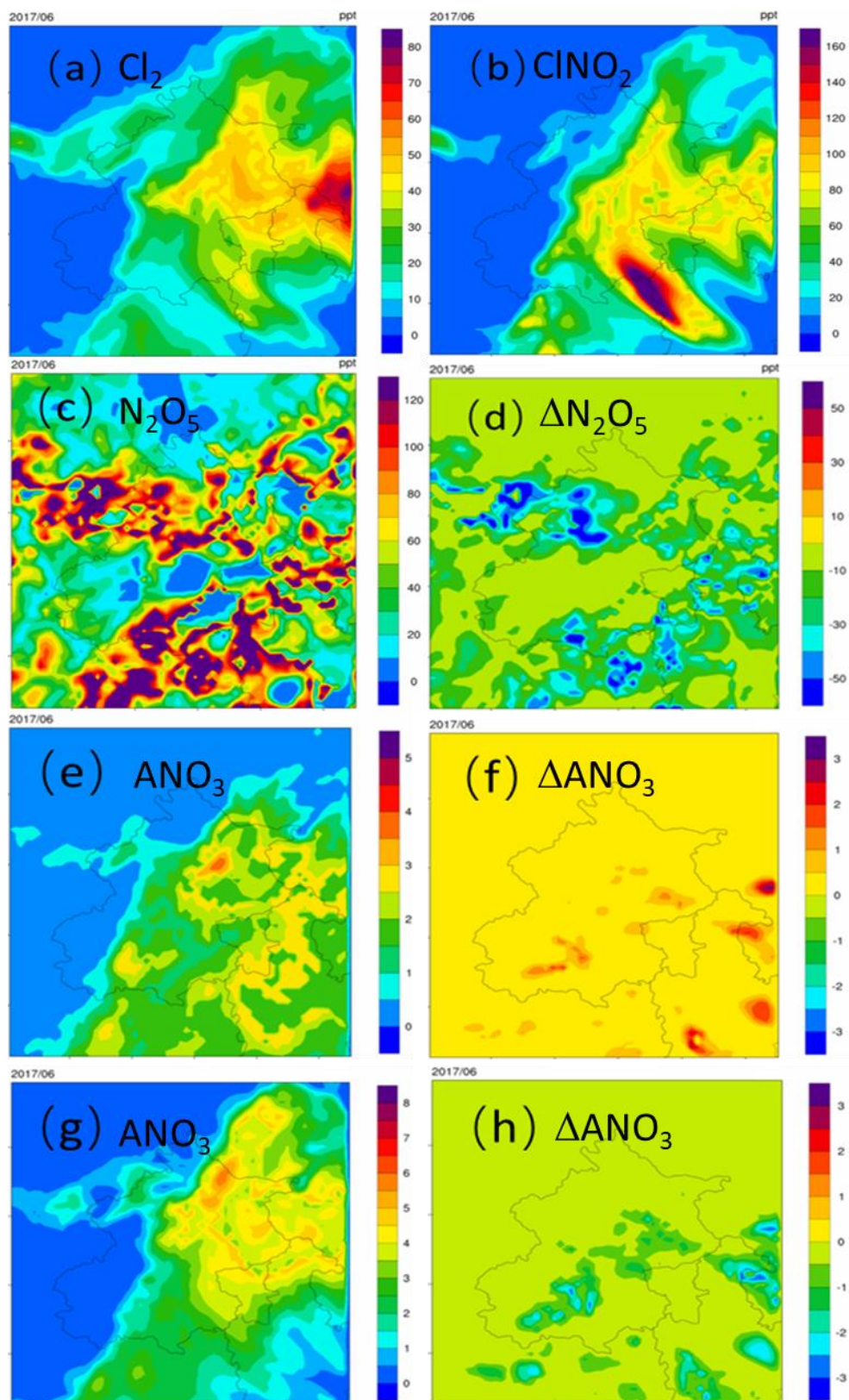
595

596 Figure 2 Comparison of observed and predicted Cl_2 and NO_3^- concentrations under

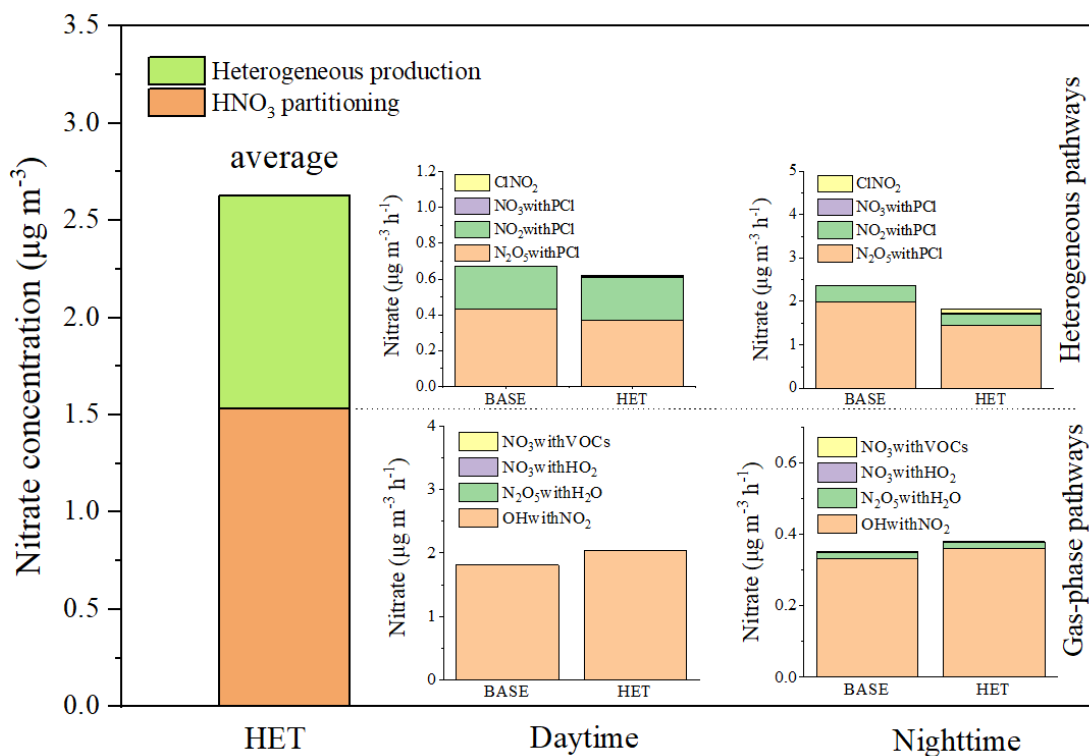
597 different uptake coefficient of O_3 (HET: daytime $\gamma_{\text{O}_3} = 1 \times 10^{-3}$, nighttime $\gamma_{\text{O}_3} =$

598 1×10^{-5} ; HET-Co: daytime $\gamma_{\text{O}_3} = 1 \times 10^{-2}$, nighttime $\gamma_{\text{O}_3} = 1 \times 10^{-4}$).

599



600
 601 Figure 3 Spatial distributions of episode-average (a) Cl_2 , (b) ClNO_2 , (c) N_2O_5 , (e)
 602 daytime nitrate (ANO_3) and (g) nighttime nitrate concentrations from 11-15 June 2017,
 603 and the differences in the episode-average (d) N_2O_5 (HET case – BASE case), (f)
 604 daytime nitrate and (g) nighttime nitrate. Units are $\mu\text{g m}^{-3}$.
 605



606
607
608
609

Figure 4 Contributions of different homogeneous and heterogeneous pathways to nitrate formation.

610 Table 1 The sectoral emissions of HCl, Cl₂ and PCl in Beijing in 2017. Unit: Mg year⁻¹

Sector	Emissions		
	HCl	Cl ₂	PCl
Power plant	22.8	1.2	6.75
Industry	587.3	20.1	89.2
Residential	202.4	8.1	34.7
Biomass burning	0.182	0	0.14
Municipal solid waste	1080.2	0	8.47
Cooking	0	0	426.8
Total	1892.9	29.4	566.1

611

612

613 Table 2 Major gas-phase and heterogeneous pathway of producing nitrate in original CMAQ and newly added or revised heterogeneous reactions
 614 in improved CMAQ.

Type	Reactions	No.	Reference	Comment
Original CMAQ				
Gas-phase chemistry	$\text{OH} + \text{NO}_2 \rightarrow \text{HNO}_3$	R1		
	$\text{N}_2\text{O}_5 + \text{H}_2\text{O} \rightarrow 2\text{HNO}_3$	R7		
	$\text{HO}_2\cdot + \text{NO}_3 \rightarrow 0.2\text{HNO}_3 + 0.8\text{OH}\cdot + 0.8\text{NO}_2$	R8		
	$\text{NO}_3 + \text{VOCs}^a \rightarrow \text{HNO}_3$	R9		
Heterogeneous chemistry	$\text{N}_2\text{O}_5(\text{g}) + \text{H}_2\text{O}(\text{aq}) \rightarrow 2\text{H}^+ + 2\text{NO}_3^-$	R5		
	$2\text{NO}_2(\text{g}) + \text{H}_2\text{O}(\text{aq}) \rightarrow \text{HONO}(\text{g}) + \text{H}^+ + \text{NO}_3^-$	R10		
Improved CMAQ				
Newly added or revised heterogeneous reactions	$\text{N}_2\text{O}_5(\text{g}) + \text{H}_2\text{O}(\text{aq}) + \text{Cl}^-(\text{aq}) \rightarrow \text{ClONO}_2(\text{g}) + \text{NO}_3^-$	R6	Bertram and Thornton (2009)	Revise R5
	$2\text{NO}_2(\text{g}) + \text{Cl}^- \rightarrow \text{ClNO}(\text{g}) + \text{NO}_3^-$	R11	Abbatt et al. (1998)	Revise R10
	$\text{NO}_3(\text{g}) + 2\text{Cl}^- \rightarrow \text{Cl}_2(\text{g}) + \text{NO}_3^-$	R12	Rudich et al. (1996)	Increase NO_3^-
	$\text{O}_3(\text{g}) + 2\text{Cl}^- + \text{H}_2\text{O}(\text{aq}) \rightarrow \text{Cl}_2(\text{g}) + \text{O}_2(\text{g}) + 2\text{OH}^-$	R13	Abbatt et al. (1998)	Affect OH
	$2\text{OH}\cdot(\text{g}) + 2\text{Cl}^- \rightarrow \text{Cl}_2(\text{g}) + 2\text{OH}^-$	R14	George et al. (2010)	Affect OH
	$\text{ClONO}_2(\text{g}) + \text{Cl}^- \rightarrow \text{Cl}_2(\text{g}) + \text{NO}_3^-$	R15	Deiber et al. (2004)	Affect OH
	$\text{HOCl}(\text{g}) + \text{Cl}^- + \text{H}^+ \rightarrow \text{Cl}_2(\text{g}) + \text{H}_2\text{O}$	R16	Pratte et al. (2006)	Affect OH
	$\text{ClONO}_2(\text{g}) + \text{Cl}^- + \text{H}^+ \rightarrow \text{Cl}_2(\text{g}) + \text{HONO}(\text{g})$ (pH < 2.0)	R17	Riedel et al. (2012)	Affect OH
	$\text{ClONO}_2(\text{g}) + \text{H}_2\text{O}(\text{aq}) \rightarrow \text{Cl}^- + \text{NO}_3^- + 2\text{H}^+$ (pH ≥ 2.0)	R18	Rossi (2003)	Increase NO_3^-

615 ^a: presents different VOCs species. In the SAPRC-11 mechanism, the VOCs species include CCHO (Acetaldehyde), RCHO (Lumped C3+
 616 Aldehydes), GLY (Glyoxal), MGLY (Methyl Glyoxal), PHEN (phenols), BALD (Aromatic aldehydes), MACR (Methacrolein), IPRD (Lumped
 617 isoprene product species).
 618

619 Table 3 Observed day (D) and night (N) NO₃⁻ concentrations (Obs.) and predicted
 620 uptake coefficient of N₂O₅ ($\gamma_{N_2O_5}$) and nitrate concentrations (Pred.) using the
 621 parameterizations of $\gamma_{N_2O_5}$ by Bertram and Thornton (2009) (Scenario 1), Davis et al.,
 622 (2008) (Scenario 2) and the upper-limit value derived by Zhou et al. (2018) (Scenario
 623 3)
 624

	NO ₃ ⁻ Obs.	Scenario1		Scenario2		Scenario3	
		$\gamma_{N_2O_5}$	Pred.	$\gamma_{N_2O_5}$	Pred.	$\gamma_{N_2O_5}$	Pred.
06/11-D	2.54	0.033	1.59	0.008	1.32	0.09	2.17
06/11-12-N	2.42	0.043	1.67	0.037	1.37	0.09	2.12
06/12-D	3.39	0.028	2.16	0.032	2.74	0.09	3.13
06/12-13-N	4.24	0.021	4.02	0.022	4.05	0.09	6.04
06/13-D	2.57	0.012	1.18	0.008	1.06	0.09	2.47
06/13-14-N	4.10	0.022	4.45	0.022	4.45	0.09	7.13
06/14-D	0.95	0.001	1.34	0.001	1.33	0.09	1.64
06/14-15-N	2.75	0.013	1.00	0.007	0.96	0.09	2.33
06/15-D	0.75	0.001	0.66	0.001	0.66	0.09	1.11

625

626